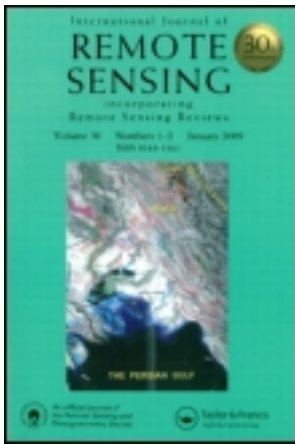


This article was downloaded by: [Fondazione Edmund Mach], [Duccio Rocchini]
On: 24 January 2012, At: 23:53
Publisher: Taylor & Francis
Informa Ltd Registered in England and Wales Registered Number: 1072954 Registered
office: Mortimer House, 37-41 Mortimer Street, London W1T 3JH, UK



International Journal of Remote Sensing

Publication details, including instructions for authors and subscription information:

<http://www.tandfonline.com/loi/tres20>

Spectral rank-abundance for measuring landscape diversity

Duccio Rocchini^a & Markus Neteler^a

^a Department of Biodiversity and Molecular Ecology, Fondazione Edmund Mach, Research and Innovation Centre, Via E. Mach 1, 38010 S. Michele all'Adige (TN), Italy

Available online: 24 Jan 2012

To cite this article: Duccio Rocchini & Markus Neteler (2012): Spectral rank-abundance for measuring landscape diversity, *International Journal of Remote Sensing*, 33:14, 4458-4470

To link to this article: <http://dx.doi.org/10.1080/01431161.2011.648286>

PLEASE SCROLL DOWN FOR ARTICLE

Full terms and conditions of use: <http://www.tandfonline.com/page/terms-and-conditions>

This article may be used for research, teaching, and private study purposes. Any substantial or systematic reproduction, redistribution, reselling, loan, sub-licensing, systematic supply, or distribution in any form to anyone is expressly forbidden.

The publisher does not give any warranty express or implied or make any representation that the contents will be complete or accurate or up to date. The accuracy of any instructions, formulae, and drug doses should be independently verified with primary sources. The publisher shall not be liable for any loss, actions, claims, proceedings, demand, or costs or damages whatsoever or howsoever caused arising directly or indirectly in connection with or arising out of the use of this material.

Technical Note

Spectral rank–abundance for measuring landscape diversity

DUCCIO ROCCHINI* and MARKUS NETELER

Department of Biodiversity and Molecular Ecology, Fondazione Edmund Mach, Research and Innovation Centre, Via E. Mach 1, 38010 S. Michele all'Adige (TN), Italy

(Received 29 November 2009; in final form 22 November 2011)

Investigation of the diversity of a landscape implies finding appropriate measures coupling information on richness and equitability. Most of the papers dealing with remotely sensed images have relied on the richness of digital numbers (DNs) or on Shannon entropy or Pielou evenness indices for measuring their heterogeneity. Instead, based on ecological theory, we will show that rank–abundance diagrams may be profitably used in remote sensing to take into account both spectral richness and spectral equitability at the same time, by using a unique approach. After a theoretical introduction to the problem, we will empirically test the proposed method by extracting DN abundances derived from a Landsat Enhanced Thematic Mapper Plus (ETM+) image representing contrasting landscapes (test sites), plotting the relative abundance of each DN value versus its rank (rank–abundance diagrams) and interpreting statistically and ecologically the achieved results. We do not propose rank–abundance diagrams as a replacement of existing measures of spectral diversity, but as a parallel method to encompass (at the same time) both richness and evenness of remotely sensed images.

1. Introduction: commonly used measures of diversity in remote sensing

It is extremely important to measure the heterogeneity of a landscape since landscape heterogeneity is strongly correlated with landscape diversity (Gillespie *et al.* 2008). Further, landscape diversity has been demonstrated to be related to the diversity at other ecosystem levels such as species diversity (e.g. Bino *et al.* 2008, He and Zhang 2009, Rocchini *et al.* 2009, St-Louis *et al.* 2009), which can thus be modelled at appropriate scales (Osborne *et al.* 2007).

While methods have mostly relied on the classification of images for landscape diversity assessment, classifying the images has several serious drawbacks: (i) the accuracy assessment involves time and cost when field assessment is involved (Foody 2002), (ii) it is difficult to build practically sound accuracy assessment protocols (Foody 2008) and (iii) there are difficulties in choosing pure training samples without any mixing effects (Small 2004, Rocchini 2010, He *et al.* 2011). Besides these technical shortcomings, classification is a subjective task by its very nature and it inevitably leads to degradation of continuous information (Palmer *et al.* 2002). Rocchini *et al.* (2009) have demonstrated that spectral richness at different spatial scales in terms of the amount

*Corresponding author. Email: duccio.rocchini@fmach.it; ducciorocchini@gmail.com

of digital numbers (hereafter DNs or even reflectance values) may be profitably used to estimate landscape diversity.

Given a certain number N of DN values, besides the use of spectral richness, the entropy can be calculated as

$$H = - \sum_{\text{DN}=1}^N P \ln(P) \quad \text{with } 0 \leq H \leq \ln(N), \quad (1)$$

where H is referred to as the Boltzmann index (Boltzmann 1872) or Shannon entropy index (Shannon and Weaver 1962), which takes into account the relative proportion P of each DN value (refer to Ricotta (2005) for major information about the use of the Shannon entropy index in remote sensing).

The Shannon entropy index takes into account the equitability of the system when it is associated with the Pielou evenness index J (Pielou 1969), calculated as

$$J = \frac{- \sum_{\text{DN}=1}^N P \ln(P)}{\ln(N)} \quad \text{with } 0 \leq J \leq 1, \quad (2)$$

which takes into account the maximum possible diversity with the same number of DNs N . Quoting Ricotta and Avena (2003), who have presented an elegant mathematical dissertation about the Pielou evenness index applied to both species and landscape classes, ‘normalisation of H with respect to maximum entropy ($J = H/H_{\max}$) is termed “evenness” because it measures deviation from an even distribution of individuals amongst the N species’.

Entropy of species communities can be easily translated to spectral diversity by considering the distribution of individual pixels among N reflectance values (DNs). As an example, consider an image composed of pixels p in the form of a matrix \mathbf{M}_p with dimension $\text{Dim}(\mathbf{M}_p) = (2,2)$ as follows:

$$\mathbf{M}_p = \begin{bmatrix} p_{11} & p_{12} \\ p_{21} & p_{22} \end{bmatrix}. \quad (3)$$

Imagine that \mathbf{M}_p is a binary matrix with two DNs (e.g. 0, 1) available. Hence, given the same richness of DNs (equalling 2), the maximum compositional diversity of this matrix is achieved when the DNs are equitably distributed in terms of their abundance as, for example, $\mathbf{M}_p = \begin{bmatrix} 1 & 1 \\ 0 & 0 \end{bmatrix}$ instead of $\mathbf{M}_p = \begin{bmatrix} 1 & 1 \\ 1 & 0 \end{bmatrix}$. The Shannon entropy index incorporates this information since it takes into account the relative proportion P of each DN within the image. In this example, the Shannon entropy index will equal 0.693 (corresponding to $\ln(2)$) versus 0.562, whereas the Pielou evenness index will equal $0.693/\ln(2)$ or $\ln(2)/\ln(2) = 1$ and $0.562/\ln(2) = 0.811$.

2. Theory beyond rank–abundance diagrams

Shannon and Pielou indices are undoubtedly powerful. However, according to Gorelick (2006), who made a critique on diversity measured by Shannon and Simpson indices, one can never capture all aspects of diversity in a single statistic. An approach that considers at the same time the richness and equitability of reflectance values in an

image would be particularly suitable for measuring remotely sensed imagery diversity. A widely used example in ecology is the rank–abundance diagrams, which are capable of graphically ‘showing the diversity’ of an array of values by plotting the abundance of each value with respect to its rank (see Magurran 1988).

Such methods have long been applied for measuring the compositional diversity of species communities considering different kinds of taxa and habitats: from phyto- and zooplankton together with fishes and macrophytes in lake ecosystems (Aoki 1995), to Collembola, Coleoptera and birds in forest ecosystems (Fattorini 2005), to post-fire chaparral plant communities (Guo and Rundel 1997).

Rank–abundance diagrams were first introduced by MacArthur (1957), who developed the theory behind the method with examples related to bird communities by plotting species abundance against ranks. Further, Whittaker (1965) straightforwardly reworked the method with a graphical representation of all possible theoretical situations of the community diversity of a species.

These diagrams are built considering the relative abundance of each species, measured as the number of individuals in an area. Once the relative abundance of a species is ordered, a rank is assigned to each species as a function of its abundance. In other words, the most common (abundant) species will have a higher number of individuals and will be ranked ‘first’. Then, abundances or relative abundances are plotted against ranks (rank–abundance diagram). Summarizing from MacArthur (1957), species are ranked from commonest to rarest along the abscissa and their abundances are plotted along the ordinate.

The application of rank–abundance diagrams to remotely sensed imagery is simple if one translates the concept of individuals to that of ‘individual pixels’ and the concept of species to that of reflectance values, as previously stressed. In fact, a species can be viewed as an attribute of each individual, like a reflectance value is an attribute of each pixel. As an example, let \mathbf{M}_p be a binary matrix of pixels p . Consider the aforementioned situations, i.e. maximum compositional diversity when $\mathbf{M}_p = \begin{bmatrix} 1 & 1 \\ 0 & 0 \end{bmatrix}$

instead of $\mathbf{M}_p = \begin{bmatrix} 1 & 1 \\ 1 & 0 \end{bmatrix}$. In the first case, the relative abundance of reflectance values ($DN = 0$ and $DN = 1$) turns out to be $A_{DN} = 0.5$ (figure 1(a)), whereas in the second case (lower compositional diversity despite the richness), the relative abundance of reflectance values turns out to be $A_{DN} = 0.75$ for $DN = 1$ and $A_{DN} = 0.25$ for $DN = 0$ (figure 1(b)).

In this case, the value $DN = 1$ having a higher abundance will obtain a lower rank with respect to $DN = 0$ (figure 1(b)). Instead, when values show equal abundances (e.g. $A_{DN} = 0.5$), their ranks are interchangeable (figure 1(a)).

3. Problems arising from the use of single diversity indices

As previously stated, using one single index of diversity may be insufficient to discriminate among different ecological situations. For instance, areas differing in richness or relative abundances of reflectance values (DNs) may show a similar Shannon index value.

As an example, let \mathbf{A} be an image composed of 10 DN values, each of which occupies a proportion equalling 0.1 of the total available area. The array of relative abundance values (A_{DN}) is thus represented by

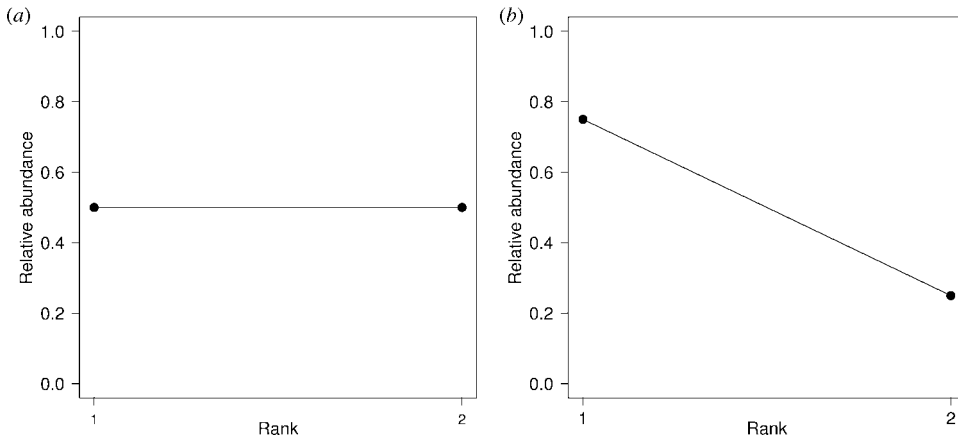


Figure 1. Theoretical example of rank–abundance diagrams derived from binary matrices \mathbf{M}_p composed of pixels p : (a) $\mathbf{M}_p = \begin{bmatrix} 1 & 1 \\ 0 & 0 \end{bmatrix}$, (b) $\mathbf{M}_p = \begin{bmatrix} 1 & 1 \\ 1 & 0 \end{bmatrix}$. We refer to the main text for major information.

$$A_{DN} = \{0.1, 0.1, 0.1, 0.1, 0.1, 0.1, 0.1, 0.1, 0.1, 0.1\}$$

with a complete equitability. Hence, the maximum possible Shannon index value with 10 classes (i.e. $\ln(10) = 2.3$) is obtained, with the maximum possible Pielou evenness index equalling 1.

Instead, let \mathbf{B} be an image with 10 DN values but with the dominance of three of them, the first of which occupies one-third of the area available. The array of relative abundance values (A_{DN}) is represented by

$$A_{DN} = \{0.3, 0.15, 0.1, 0.06, 0.06, 0.06, 0.06, 0.06, 0.06, 0.06\}.$$

In this case, the Shannon index, as well as the Pielou evenness index, would not be far from its maximum value (equalling 2.11 and 0.92, respectively). This is mainly related to the fact that the Shannon index contains a logarithmic function (see equation (1)), thus being more sensitive to rare values, i.e. to richness instead of relative abundance (Nagendra 2002).

Finally, consider a completely different situation (referred to as image C) with a higher richness (200 DN values) and a very low evenness, for example, with one dominant DN value occupying 70% of the area. The array of relative abundance values (A_{DN}) turns out to be

$$A_{DN} = \{0.7, 0.0015, 0.0015, 0.0015, 0.0015, 0.0015, 0.0015, 0.0015, \dots, 0.0015\}.$$

Although image C is very different from the aforementioned images A and B in terms of richness and relative abundance, the Shannon index is very similar (equalling 2.2 even if it is far from its possible maximum value equalling $\ln(200) = 5.3$), albeit the Pielou evenness index reveals unequitability, equalling 0.41.

The presented cases are related to extreme theoretical situations, but also in empirical studies, it is sometimes difficult to straightforwardly detect differences in richness

and relative abundances between two or more images. Although the Pielou evenness index may reveal differences among the aforementioned images (A, B and C), which are not distinguishable in terms of Shannon-based diversity, rank–abundance diagrams may represent a more straightforward method for immediately figuring out the richness and the relative abundance of reflectance values in an area. In fact, both richness (on the x -axis) and relative abundance (y -axis) are explicitly taken into account in a rank–abundance diagram.

Figure 2 represents rank–abundance diagrams derived from the aforementioned examples, passing from high (figure 2(a) and (b)) to low equitability (figure 2(c)). The higher the richness, the higher will be the dimensionality of the x -axis (figure 2(c)), whereas the higher the equitability, the lower will be the slope of the rank–abundance trend (figure 2(a) and (b)).

Rank–abundance diagrams may have different shapes (e.g. broken stick, log normal, log series, geometric series; refer to Magurran (1988)), but generally the attained curve is divisible into three parts (when plotted using a log scale that decreases outlier effect; see Section 4.2): (i) a first part with a high slope related to a few dominant reflectance values each related to land-use classes that occupy most of the landscape (e.g. wheat crops in the case of a highly heterogeneous landscape or the sea in an intermediately heterogeneous landscape), (ii) a middle less steep part related to several intermediately dominating DNs related to, for example, seminatural areas and (iii) a terminal part related to a few rare DNs. That is why this curve has been named a ‘sigmoid rank–abundance curve’, which is typical of heterogeneous communities and landscapes (see Whittaker (1965) and references therein). Instead, quasi-linear geometric series are typical of homogeneous systems since there are only a very limited number of DN values (low richness) and a few of these are extremely dominant. We refer to Magurran (1988) for a comprehensive description of all the possible empirical shapes of rank–abundance diagrams attained with real ecological data.

As far as we know, no efforts have been made previously to apply rank–abundance diagrams to remotely sensed images. The aim of this article is to test the potential of rank–abundance diagrams in investigating the spectral diversity of satellite imagery.

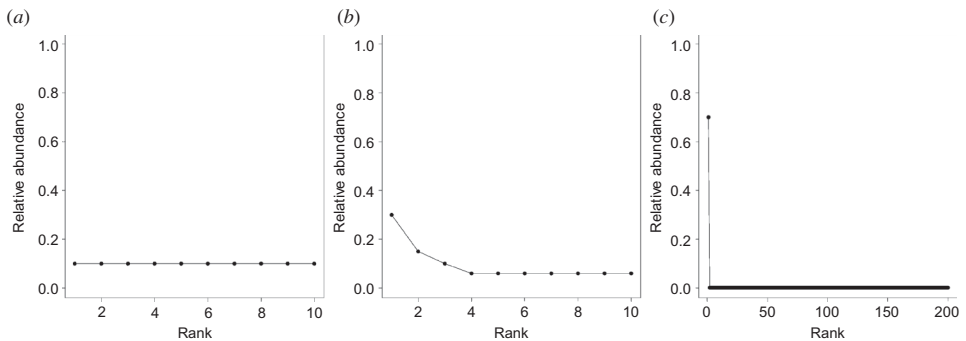


Figure 2. Rank–abundance diagrams derived from three different situations. (a) Array A: richness = 10 DN values, complete equitability. (b) Array B: richness = 10 DN values, with 3 values being more abundant. (c) Array C: richness = 200 DN values, with 1 dominant DN value. Notice that although the images are different in terms of richness or relative abundance, the Shannon entropy index H is very similar equalling 2.3, 2.11 and 2.2 for images (a), (b) and (c), respectively. We refer to the main text for major explanations.

In particular, we will empirically test the method by (i) extracting DN abundances from contrasting landscapes (test sites), (ii) plotting the relative abundance of each DN value versus its rank and (iii) interpreting statistically and ecologically the achieved rank–abundance diagrams.

4. Empirical test

4.1 Test site and data acquisition

In order to test the potential of rank–abundance diagrams in discriminating different landscapes with different levels of heterogeneity, we selected a Mediterranean area (Tuscany, Italy) due to its known gradient in land-use heterogeneity (e.g. Marignani *et al.* 2008, Geri *et al.* 2010), ranging from very homogeneous areas (e.g. sea) to very heterogeneous typical landscapes with a complex mosaic of urban areas and crops mixed with seminatural areas and forests.

A Landsat Enhanced Thematic Mapper Plus (ETM+) image (path 192, row 030, acquisition date 20 June 2000, spatial resolution 28.5 m, bands from 1 to 5 and 7; see figure 3(a)) was acquired from the Global Land Cover Facility site hosted by the University of Maryland (<http://glcf.umd.edu/>; see Tucker *et al.* (2004) for

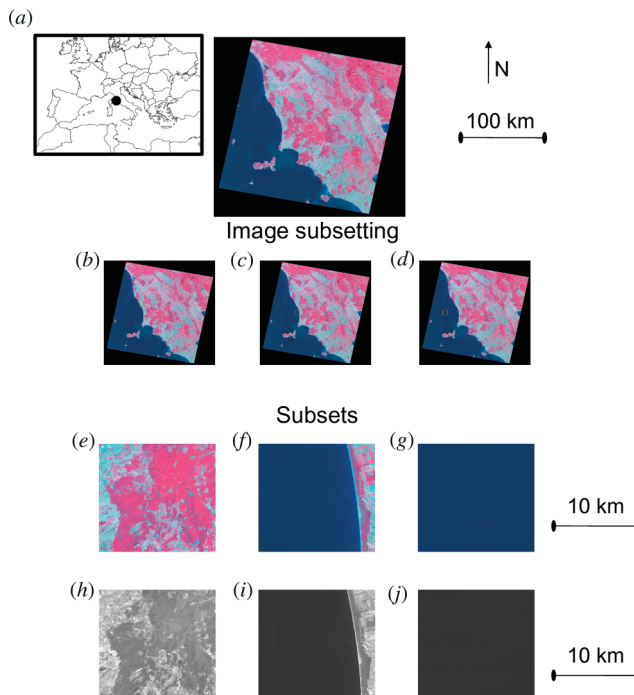


Figure 3. Landsat ETM+ image covering Tuscany, Italy (path 192, row 030, (a)). Three subsets of the image were selected based on three differently heterogeneous landscapes: a highly heterogeneous landscape with high DN richness and equitability ((b), (e), (h)); an intermediately heterogeneous landscape with high DN richness but low equitability ((c), (f), (i)); a highly homogeneous landscape with low DN richness and low equitability ((d), (g), (j)). Three subsets were selected showing three different heterogeneous landscapes. Rank–abundance diagrams were derived using the first principal component of each subset ((h), (i), (j)). We refer to the main text for major information.

major details). We refer to Nagendra and Rocchini (2008) for a complete list of sites with freely available images with different spatial and spectral resolution.

In order to speed up the analysis, we selected three subsets of the image (figure 3(b)–(d)) with a window size of 10 km × 10 km (ca. 350 × 350 pixels) with known different degrees of spectral heterogeneity: (i) a highly heterogeneous landscape mainly composed of Mediterranean forests dominated by oak species like *Quercus pubescens* (downy oak) interspersed with seminatural vegetation dominated by shrub cover intermingled with seminatural grasslands and wheat crops (figure 3(e)), (ii) an intermediately heterogeneous landscape, containing the previous classes (with *Q. ilex*, holly oak, dominating with respect to *Q. pubescens*), but with an additional class (sea) clearly dominating with respect to the others (figure 3(f)) and (iii) a highly homogeneous landscape, containing only the sea as land-cover class (figure 3(g)).

Theoretically, the three selected areas differed from each other considering both DN richness and equitability. In fact, the so-called highly heterogeneous landscape had potentially a high number of possible DNs (high richness) with a high evenness due to the same relative occupancy of the different land-use classes. The ‘intermediately heterogeneous landscape’ showed potentially a high richness but with a lower equitability due to the presence of a clearly dominating class (the sea). Finally, the ‘highly homogeneous landscape’ showed a very low richness with an expected dominance of a few DN values.

4.2 Building rank–abundance diagrams

Notice that rank–abundance diagrams are based on a one-dimensional matrix (the aforementioned \mathbf{M}_p) from which the abundance of each DN in one band is calculated.

Thus, before building rank–abundance diagrams, one should choose a single band to work with. Following biological theory, an infrared waveband should be used when working with vegetation because of its intrinsic capability of discriminating different vegetation types (Rocchini 2007). An alternative is to use data reduction methods such as principal component analysis (PCA). In this article, an unstandardized PCA was applied to the image by retaining the first principal component (PC1) explaining 86.53% of the variance.

It is noteworthy that PCA output is a band with continuous values different from each other, thus threatening abundance-based calculation. For this reason, PC1 was converted into an 8-bit band splitting values into 256 equal intervals, hereafter simply referred to as DN values (figure 3(h)–(j)). Table 1 summarizes the aforementioned differences in richness (number of DNs) and equitability (in terms of both Shannon H and Pielou J) of the three selected landscapes using the DN values of the first principal component. Heterogeneous landscapes had a high DN richness but a different degree of equitability, whereas the highly homogeneous landscape had a low richness and a low equitability (table 1).

For each landscape, rank–abundance diagrams were derived as follows: (i) the abundance of each DN value in the first principal component was calculated, (ii) DNs were ranked, with the most abundant DN ranked first and (iii) abundance was plotted against ranks. Relative abundances were used in order to be consistent with previous studies using rank–abundance diagrams (see Magurran 1988). According to MacArthur (1957), DN abundance was plotted even on a log scale in order to decrease the outlier effect, that is, the smoothing of the curve due to hyper-dominant DN values (see next section).

Table 1. Statistics concerning the three sample sites selected.

Landscape complexity	Richness	Shannon entropy (H)	Pielou evenness (J)
Highly heterogeneous landscape	177	4.59	0.89
Intermediately heterogeneous landscape	196	3.24	0.61
Highly homogeneous landscape	16	1.75	0.63

4.3 Results

The highly heterogeneous landscape showed a rank–abundance trend with a very low slope (figure 4(a)). On the contrary, the negative slope rose up passing through the intermediately heterogeneous (figure 4(b)) landscape until becoming very high for the highly homogeneous landscape (figure 4(c)).

Richness, i.e. the number of possible DN values (corresponding to the number of ranks in the x -axis), showed a slight decrease passing from the heterogeneous landscape to the homogeneous one (see table 1 and figure 4). Hence, besides the relative abundance of DN values, even DN richness contributed to the aforementioned increase of the slope passing from a heterogeneous to a homogeneous landscape.

Concerning the tails of the curve, representing dominant (left tail) and rare (right tail) DN values, the highly heterogeneous landscape showed a strong right-sided tail, which was conserved even when log values were plotted, indicating a general equitability of the distribution of the abundances of values. The first point of the curve, roughly corresponding to wheat crops, albeit it representing the dominant DN value, showed a very low dominance corresponding to ca. 5% of the total abundance. The fact that the dominant DN value has a very low abundance means that a highly interspersed landscape mosaic exists since a dominant land use cannot be discerned (see figure 3).

This pattern reversed once the homogeneous landscape was considered with the maintenance of only a few dominant DN values. The relative abundance of the dominant DN value of ca. 27% of the total abundance means that in the homogeneous landscape, one single DN value occupied up to one-third of the entire image being considered.

The log transformation of the relative abundance of DN values led to sigmoid (heterogeneous landscapes; figure 4(d) and (e)) versus linear (homogeneous landscape; figure 4(f)) trends.

5. Discussion

Differently heterogeneous landscapes showed marked differences in the rank–abundance diagrams of the reflectance values. As stressed by Guo and Rundel (1997), the most appropriate approaches for measuring diversity must be capable of detecting subtle differences between sites. In this view, rank–abundance diagrams are powerful tools to investigate the richness- and composition-based diversity of a landscape since they straightforwardly account for both (i) richness, measured as the number of ranks, i.e. by the length of the x -axis, and (ii) equitability, derived from the slope of

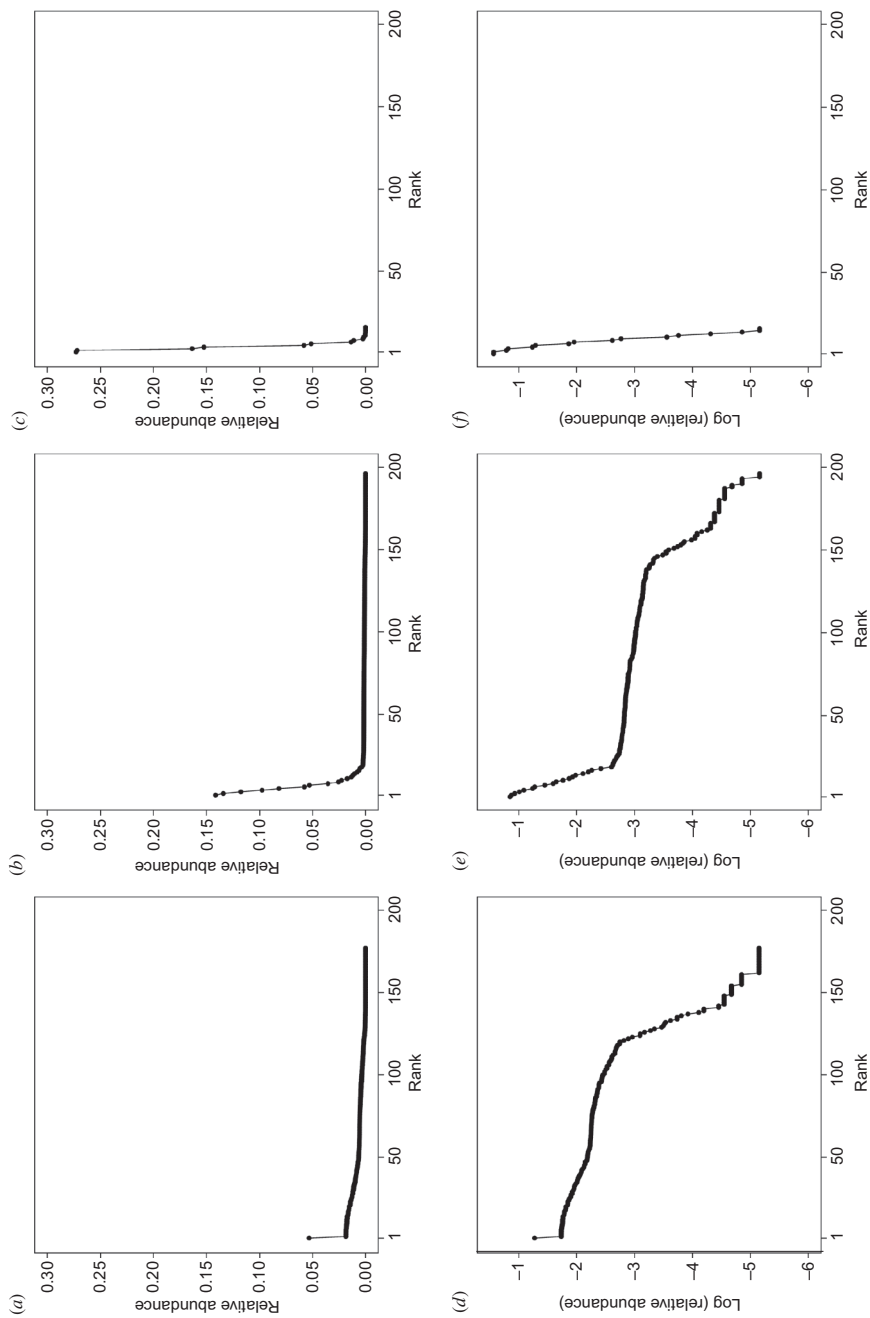


Figure 4. Rank-abundance diagrams for the three different heterogeneous landscapes (see figure 3): a highly heterogeneous landscape, considering relative abundances (a), and relative abundances on a logarithmic scale (d); an intermediately heterogeneous landscape, considering relative abundances (b), and relative abundances on a logarithmic scale (e); a highly homogeneous landscape, considering relative abundances (c), and relative abundances on a logarithmic scale (f). Notice that the negative slope of the diagram becomes higher, whereas the landscape becomes more homogeneous, indicating a lower richness and equitability in the reflectance values.

the rank–abundance curves, i.e. the higher the slope, the lower the equitability of the system.

Therefore, the main strength of rank–abundance diagrams is that they allow us to maintain the information relative to the distribution of the values being considered (i.e. species or reflectance data) without any loss of detail since every single abundance is explicitly shown (McGill *et al.* 2007).

Moreover, each part of a rank–abundance diagram conveys different information, thus allowing investigation of the distribution of diversity values over a landscape. As an example, according to Murray and Westoby (2000), the tails (left and right) of a rank–abundance curve represent dominant and rare (i.e. sparse everywhere) values, respectively. Therefore, it is expected that landscapes with higher diversity should show a longer tail skewed towards the right (figures 4(a) and (b)), whereas homogeneous landscapes should show a longer left-skewed tail increasing their slope (figure 4(c)). When transforming abundance to a log scale, the right-skewed queue should remain visible in the case of high landscape heterogeneity, whereas it should disappear for more homogeneous landscapes (see Murray *et al.* 1999). That is why the highly heterogeneous landscape showed a right-skewed tail persistent even with abundance represented on a log scale (figure 4(d)). This right-skewed tail fell down more steeply in the case of the intermediately heterogeneous landscape (figure 4(e)). Finally, it definitely disappeared for the highly homogeneous landscape (figure 4(f)).

Rank–abundance diagrams have long been applied for testing very different ecological hypotheses, e.g. estimating the species diversity of different plant structural layers (trees, shrubs and herbs; see Yin *et al.* 2005), investigating the dispersal limitation of meta-communities (Hubbel 2001), fitting different kinds of functions to species abundance distribution (McGill 2003) or testing patterns of species abundance distribution considering different elevational bands (McGill *et al.* 2007).

All the aforementioned examples are concerned with species diversity. It is worth stressing that species are modelled as ‘pure’ (i.e. objectively identified) entities, although some concerns exist, mainly related to taxonomic inflation (see Isaac *et al.* 2004, Knapp *et al.* 2005) and observer bias (Nimis 2001, Bacaro *et al.* 2009). Instead, pixels are expected to be mixed in their very nature (Small 2004), leading to a higher uncertainty in the discrimination among different areas (Rocchini 2010). However, it has been demonstrated in the ecological literature that methods used to measure species diversity also apply to remotely sensed imagery diversity (see, e.g. Rocchini (2007), Bino *et al.* (2008), He and Zhang (2009) and St-Louis *et al.* (2009) for some empirical examples and Gillespie *et al.* (2008) and Nagendra and Rocchini (2008) for a review on the matter). Moreover, as stressed by Aoki (1995), the approaches used for measuring diversity can be applied not only to species but also to all those characters showing distributions. This is definitely the case for spectral values, whose statistical distribution may directly reflect the ecological distribution of different habitats over a landscape.

Of course, the proposed method is not free from drawbacks. As an example, given the same spectral properties of the images being used, area effects should thus be seriously taken into account. It is obvious that the higher the area being sampled, the higher will be the probability of obtaining a higher number of DN's (i.e. ranks, until a maximum of 256 in the case of an 8-bit imagery) since bigger areas are expected to contain a higher number of habitats that should show different reflectances from each other. Recalling the ecological theory from which rank–abundance diagrams derive, the relative abundance of each species in a sample varies with sample size unless the

spatial distribution of individuals is uniform (Kobayashi 1980). Hence, a comparison of two landscapes A and B sampled with a different sample size (extent) may lead to misleading results. In fact, if $S_A > S_B$ with $S = \text{extent}$, the diversity of A may be overestimated simply because of its larger size.

6. Conclusions

In this article, we have presented a method for comparing the diversity of different landscapes based on rank–abundance diagrams of spectral reflectance. We have presented the diagrams from both a theoretical and an empirical point of view. There is a need for finding new ways to calculate satellite imagery heterogeneity accounting for (i) spectral richness, e.g. the number of DNs in an image, and (ii) spectral evenness, i.e. spectral equitability. Rank–abundance diagrams incorporate both types of information. Hence, they are a robust but straightforward approach for estimating and comparing the heterogeneity of satellite images of different areas.

As a cautionary remark, it is worth noting that we do not propose rank–abundance diagrams as a replacement of existing measures of spectral diversity, but as a parallel method to encompass (and explicitly account for) both richness and evenness by means of a unique approach. That is why we chose highly contrasting landscapes with known differences in richness and abundance for empirically testing the method. Further research will disentangle the potential of the proposed approach by (i) estimating the ecological relevance of spectral rank–abundance by correlating it with field biological data (species-based rank–abundance), (ii) performing multi-scale analysis and testing the sensitivity to scale variation of spectral rank–abundance and (iii) considering different sensors with different spatial, spectral and radiometric resolutions.

Acknowledgements

We are grateful to the handling editor S. Tanaka and to an anonymous referee for their comments on a previous version of this article. D.R. is partially funded by the Autonomous Province of Trento (Italy) ACE-SAP project (regulation number 23, 12 June 2008, of the University and Scientific Research Service). This study has been partially funded by the Earth and Space Foundation Award (<http://www.earthandspace.org/>).

References

- AOKI, I., 1995, Diversity and rank–abundance relationship concerning biotic compartments. *Ecological Modelling*, **82**, pp. 21–26.
- BACARO, G., BARAGATTI, E. and CHIARUCCI, A., 2009, Using taxonomic data to assess and monitor biodiversity: are the tribes still fighting? *Journal of Environmental Monitoring*, **11**, pp. 798–801.
- BINO, G., LEVIN, N., DARAWSHI, S., VAN DER HAL, N., REICH-SOLOMON, A. and KARK, S., 2008, Landsat derived NDVI and spectral unmixing accurately predict bird species richness patterns in an urban landscape. *International Journal of Remote Sensing*, **29**, pp. 3675–3700.
- BOLTZMANN, L., 1872, Weitere Studien über das Wärmegleichgewicht unter Gasmolekülen. *Wiener Berichte*, **66**, pp. 275–370.

- FATTORINI, S., 2005, A simple method to fit geometric series and broken stick models in community ecology and island biogeography. *Acta Oecologica*, **28**, pp. 199–205.
- FOODY, G.M., 2002, Status of land cover classification accuracy assessment. *Remote Sensing of Environment*, **80**, pp. 185–201.
- FOODY, G.M., 2008, Harshness in image classification accuracy assessment. *International Journal of Remote Sensing*, **29**, pp. 3137–3158.
- GERI, F., AMICI, V. and ROCCHINI, D., 2010, Human activity impact on the heterogeneity of a Mediterranean landscape. *Applied Geography*, **30**, pp. 370–379.
- GILLESPIE, T.W., FOODY, G.M., ROCCHINI, D., GIORGI, A.P. and SAATCHI, S., 2008, Measuring and modelling biodiversity from space. *Progress in Physical Geography*, **32**, pp. 203–221.
- GORELICK, R., 2006, Combining richness and abundance into a single diversity index using matrix analogues of Shannon's and Simpson's indices. *Ecography*, **29**, pp. 525–530.
- GUO, Q. and RUNDEL, P.W., 1997, Measuring dominance and diversity in ecological communities: choosing the right variables. *Journal of Vegetation Science*, **8**, pp. 405–408.
- HE, K. and ZHANG, J., 2009, Testing the correlation between beta diversity and differences in productivity among global ecoregions, biomes, and biogeographical realms. *Ecological Informatics*, **4**, pp. 93–98.
- HE, K.S., ROCCHINI, D., NETELER, M. and NAGENDRA, H., 2011, Benefits of hyperspectral remote sensing for tracking plant invasions. *Diversity and Distributions*, **17**, pp. 381–392.
- HUBBEL, S.P., 2001, *The Unified Neutral Theory of Biodiversity and Biogeography* (Princeton, NJ: Princeton University Press).
- ISAAC, N.J.B., MACE, G.M. and MALLET, J., 2004, Taxonomic inflation: its influence on macroecology and conservation. *Trends in Ecology and Evolution*, **19**, pp. 464–469.
- KNAPP, S., LUGHADHA, E.N. and PATON, A., 2005, Taxonomic inflation, species concepts and global species lists. *Trends in Ecology and Evolution*, **20**, pp. 7–8.
- KOBAYASHI, S., 1980, A model of the species rank–abundance relation for a community in an open habitat. *Researches on Population Ecology*, **22**, pp. 51–68.
- MACARTHUR, R.H., 1957, On the relative abundance of bird species. *Proceedings of the National Academy of Sciences of the United States of America*, **43**, pp. 293–295.
- MAGURRAN, A.E., 1988, *Ecological Diversity and Its Assessment* (Princeton, NJ: Princeton University Press).
- MARIGNANI, M., MACCHERINI, S., ROCCHINI, D., CHIARUCCI, A. and TORRI, D., 2008, Planning restoration in a cultural landscape in Italy using object-based approach and historical analysis. *Landscape and Urban Planning*, **84**, pp. 28–37.
- MCGILL, B.J., 2003, A test of the unified neutral theory of biodiversity. *Nature*, **422**, pp. 881–885.
- MCGILL, B.J., ETIENNE, R.S., GRAY, J.S., ALONSO, D., ANDERSON, M.J., BENECHA, H.K., DORNELAS, M., ENQUIST, B.J., GREEN, J.L., HE, F., HURLBERT, A.H., MAGURRAN, A.E., MARQUET, P.A., MAURER, B.A., OSTLING, A., SOYKAN, C.U., UGLAND, K.I. and WHITE, E.P., 2007, Species abundance distributions: moving beyond single prediction theories to integration within an ecological framework. *Ecology Letters*, **10**, pp. 995–1015.
- MURRAY, B.R., RICE, B.L., KEITH, D.A., MYERSCOUGH, P.J., HOWELL, J., FLOYD, A.G., MILLS, K. and WESTOBY, M., 1999, Species in the tail of rank–abundance curves. *Ecology*, **80**, pp. 1806–1816.
- MURRAY, B.R. and WESTOBY, M., 2000, Properties of species in the tail of rank–abundance curves: the potential for increase in abundance. *Evolutionary Ecology Research*, **2**, pp. 583–592.
- NAGENDRA, H., 2002, Opposite trends in response for the Shannon and Simpson indices of landscape diversity. *Applied Geography*, **22**, pp. 175–186.
- NAGENDRA, H. and ROCCHINI, D., 2008, High resolution satellite imagery for tropical biodiversity studies: the devil is in the detail. *Biodiversity and Conservation*, **17**, pp. 3431–3442.

- NIMIS, P.L., 2001, A tale from Bioutopia. *Nature*, **413**, p. 21.
- OSBORNE, P.E., FOODY, G.M. and SUAREZ-SEOANE, S., 2007, Non-stationarity and local approaches to modelling the distributions of wildlife. *Diversity and Distributions*, **13**, pp. 313–323.
- PALMER, M.W., EARLS, P., HOAGLAND, B.W., WHITE, P.S. and WOHLGEMUTH, T., 2002, Quantitative tools for perfecting species lists. *Environmetrics*, **13**, pp. 121–137.
- PIELOU, E.C., 1969, *An Introduction to Mathematical Ecology* (New York: John Wiley).
- RICOTTA, C., 2005, On possible measures for evaluating the degree of uncertainty of fuzzy thematic maps. *International Journal of Remote Sensing*, **26**, pp. 5573–5583.
- RICOTTA, C. and AVENA, G.C., 2003, On the relationship between Pielou's evenness and landscape dominance within the context of Hill's diversity profiles. *Ecological Indicators*, **2**, pp. 361–365.
- ROCCHINI, D., 2007, Effects of spatial and spectral resolution in estimating ecosystem [alpha]-diversity by satellite imagery. *Remote Sensing of Environment*, **111**, pp. 423–434.
- ROCCHINI, D., 2010, While Boolean sets non-gently rip: a theoretical framework on fuzzy sets for mapping landscape patterns. *Ecological Complexity*, **7**, pp. 125–129.
- ROCCHINI, D., RICOTTA, C., CHIARUCCI, A., DE DOMINICIS, V., CIRILLO, I. and MACCHERINI, S., 2009, Relating spectral and species diversity through rarefaction curves. *International Journal of Remote Sensing*, **30**, pp. 2705–2711.
- SHANNON, C.E. and WEAVER, W., 1962, *The Mathematical Theory of Communication* (Urbana, IL: University of Illinois Press).
- SMALL, C., 2004, The Landsat ETM+ spectral mixing space. *Remote Sensing of Environment*, **93**, pp. 1–17.
- ST-LOUIS, V., PIDGEON, A.M., CLAYTON, M.K., LOCKE, B.A., BASH, D. and RADELOFF, V.C., 2009, Satellite image texture and a vegetation index predict avian biodiversity in the Chihuahuan Desert of New Mexico. *Ecography*, **32**, pp. 468–480.
- TUCKER, C.J., GRANT, D.M. and DYKSTRA, J.D., 2004, NASA's global orthorectified Landsat data set. *Photogrammetric Engineering & Remote Sensing*, **70**, pp. 313–322.
- WHITTAKER, R.H., 1965, Dominance and diversity in land plant communities. *Science*, **147**, pp. 250–260.
- YIN, Z.-Y., REN, H., ZHANG, Q.-M., PENG, S.-L., GUO, Q.-F. and ZHUO, G.Y., 2005, Species abundance in a forest community in south China: a case of Poisson lognormal distribution. *Journal of Integrative Plant Biology*, **47**, pp. 801–810.